

## Hole formation and growth in freely standing polystyrene films

K. Dalnoki-Veress, B.G. Nickel, C. Roth, and J.R. Dutcher\*

*Department of Physics and the Guelph-Waterloo Program for Graduate Work in Physics, University of Guelph, Guelph, Ontario, Canada N1G 2W1*

(Received 12 May 1998)

Using optical microscopy, we have measured the formation and growth of holes in freely standing polystyrene films in the melt state. For all films, we observed exponential growth of the hole radius and uniform thickening. Our measurements are interpreted in terms of the dependence of the viscosity on the shear strain rate associated with the hole growth process. The measurement of hole growth in thin freely standing polymer films provides a unique probe of nonlinear viscoelastic effects in confined polymers.  
[S1063-651X(99)11002-X]

PACS number(s): 68.15.+e, 68.60.Dv, 83.50.Gd

Recently, there have been many experimental and theoretical studies of the mobility of polymer molecules in confined geometries. Changes in mobility due to perturbations of the equilibrium conformation of molecules, interactions with confining material, and the thermal stability of the molecules are of particular interest (see Refs. [1–11], and references therein). Measurement of the mobility of polymer molecules confined within thin films at different temperatures provides a direct probe of the thermal stability of thin films. For films supported on substrates, thermal instabilities can lead to dewetting [1–3,8], producing nonuniform film coverage. For unsupported or freely standing films, thermal instabilities can lead to the formation of holes, i.e., rupture [4,10]. A fundamental understanding of dewetting and rupture is important for the use of thin polymer films in technological applications.

There are two mechanisms for hole formation in thin polymer films in the melt state: nucleation, and spontaneous hole formation. The nucleation and growth of holes in thick (film thickness  $5 < h < 50 \mu\text{m}$ ) freely standing polydimethylsiloxane films was studied in the pioneering work of Debrégeas *et al.* [4,10]. Evidence for linear viscoelastic behavior of the films was inferred from the observed exponential growth of the hole radius and the uniform thickening of the films during hole growth. This behavior is qualitatively different from hole formation in less viscous systems in which inertia plays an important role.

In the present manuscript, we describe the results of our measurements of spontaneous and nucleated hole formation and growth in freely standing polystyrene (PS) films with thicknesses  $96 \text{ nm} < h < 372 \text{ nm}$ . The hole growth measurements were performed at a fixed measurement temperature  $T = 115^\circ\text{C}$  which is only  $\sim 18^\circ\text{C}$  greater than the bulk value of the glass transition temperature  $T_g = (97 \pm 2)^\circ\text{C}$ . As a result, the viscosity values were very large compared with those studied in Refs. [4,10]. As in the work of Debrégeas *et al.* [4,10], we observe exponential growth of the hole radius and uniform thickening of the films during hole growth for both spontaneous and nucleated holes. By measuring the characteristic growth time  $\tau$  as a function of film thickness  $h$  in this very simple experiment, we have obtained a measure

of the viscosity  $\eta$  at the edge of the hole. We find that  $\eta$  decreases with decreasing thickness  $h$ , which can be understood in terms of the dependence of  $\eta$  on the shear strain rate  $\dot{\gamma}$  associated with the hole growth process.

Polystyrene molecules (molecular weight  $\bar{M}_w = 767,000$ ; polydispersity index  $\bar{M}_w/\bar{M}_n = 1.10$ ) from Polymer Source Inc. were dissolved in toluene with PS concentrations (by mass) ranging from 2.0% to 3.7%. The solutions were filtered ( $0.2 \mu\text{m}$  pore size) and spin coated onto clean glass slides using a spin speed of either 3000 or 4000 rpm. The PS films on the glass slides were annealed under vacuum at a temperature  $T = 110^\circ\text{C}$  ( $> T_g$ ) for 12 h. This removes residual solvent molecules which can act as plasticizers and allows relaxation of the chains since the annealing time is many orders of magnitude larger than the reptation time at the annealing temperature. The films were cooled to room temperature at a constant, slow rate ( $1^\circ\text{C}/\text{min}$ ), ensuring a well-defined thermal history. The PS films were then floated onto a water surface, captured across a 4-mm-diameter hole in a stainless steel holder, and dried in air. For the present study, we made a series of 25 films ranging in thickness from 96 nm to 372 nm, as measured using ellipsometry. For this range of film thicknesses,  $T_g$  is equal to that in bulk.

There were two ways in which holes formed in the freely standing PS films. First, when the films were heated to temperatures  $T > T_g$ , holes formed spontaneously either by a process analogous to spinodal decomposition [1] or by nucleation by dust spots smaller than the spatial resolution of the microscope ( $\sim 0.2 \mu\text{m}$ ). We have also purposely nucleated holes in room-temperature PS films using a heated, electrochemically etched tungsten scanning tunneling microscope tip onto which we have evaporated a thin layer ( $\sim 100 \text{ nm}$  thick) of silicon oxide ( $\text{SiO}_x$ ) [5]. By bringing the heated tip (temperature  $T > T_g$ ) into brief contact with the films, we have successfully nucleated holes with radii as small as  $0.1 \mu\text{m}$ . The  $\text{SiO}_x$  layer discourages adhesion between the tip and the film and results in circular holes with a uniform hole edge as viewed using optical microscopy. The films were placed in an optical microscope hot stage and heated at a rate of  $5\text{--}10^\circ\text{C}/\text{min}$  to  $T = 115^\circ\text{C}$ . At this fixed sample temperature, the hole radius was measured as a function of time using an optical imaging system consisting of a reflected-light microscope, charge-coupled device camera, and image analysis system.

\*Author to whom correspondence should be addressed.

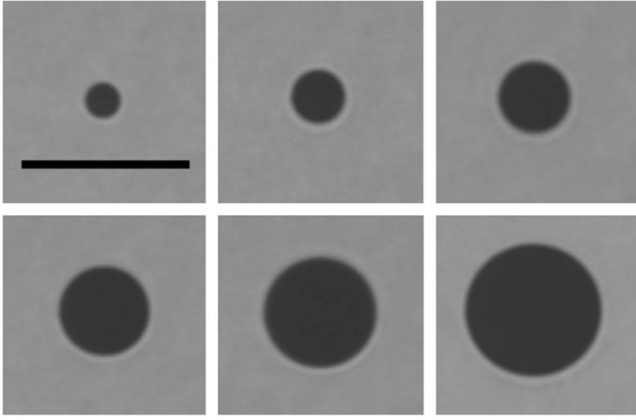


FIG. 1. Sequence of images for hole growth in a freely standing PS film with  $h=96$  nm at  $T=115$  °C. The bar in the first image is 20  $\mu\text{m}$  long, and the magnification is the same for all images. The time between successive images is 60 s.

In Fig. 1 is shown a sequence of images for the growth of a hole in a PS film with  $h=96$  nm. The process occurs very slowly because of the large values of viscosity for the polymer at the measurement temperature. Typically, the velocity with which the hole radius increases is tens of nm/s which is about nine orders of magnitude less than the growth velocity for the rupture of soap films [12].

Figure 2 is a plot of the natural logarithm of the hole radius  $\mathcal{R}$ , normalized to the value of the radius  $\mathcal{R}_0$  first measured for each hole, as a function of time for six representative films ranging in film thickness from  $h=96$  nm to 372 nm. For the data shown in Fig. 2, holes were nucleated in the two thickest films since holes did not form spontaneously during the experiment; holes formed spontaneously for the thinner films. For all hole growth experiments, the temperature was fixed at  $T=115$  °C. At this measurement temperature, hole growth in films with  $h<96$  nm occurred too fast to obtain reliable data. For each film thickness, the initial

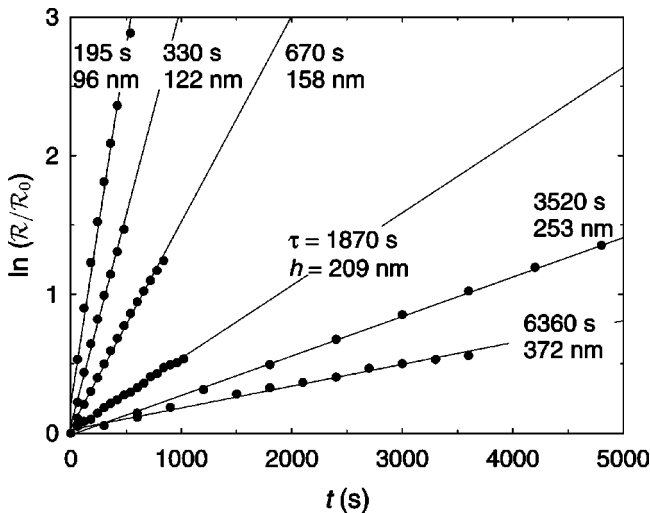


FIG. 2. Natural logarithm of the hole radius  $\mathcal{R}$ , normalized to the value of the radius  $\mathcal{R}_0$  first measured for each hole, as a function of time for six representative PS films ranging in film thickness from  $h=96$  nm to 372 nm. The  $\tau$  and  $h$  values are listed for each data set.

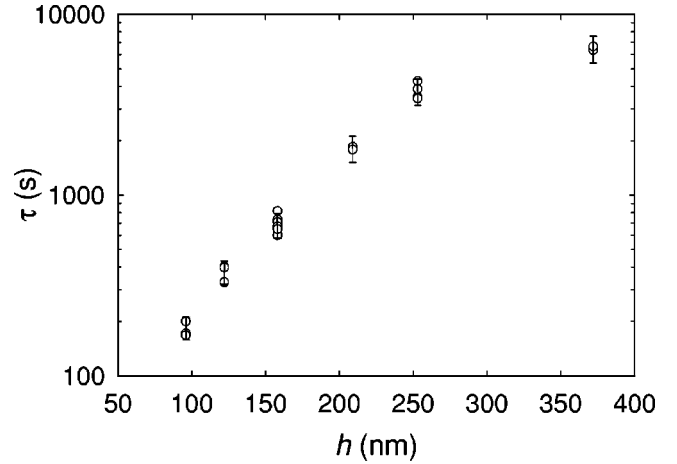


FIG. 3. Time constant  $\tau$ , which characterizes the growth rate of the holes at  $T=115$  °C, versus PS film thickness  $h$ .

dependence of  $\ln(\mathcal{R}/\mathcal{R}_0)$  versus time  $t$  is linear, corresponding to exponential growth of the hole radius

$$\mathcal{R}(t) = \mathcal{R}_0 e^{t/\tau}, \quad (1)$$

where  $\tau$  is the time which characterizes the growth of the hole. For each value of the film thickness, we prepared multiple samples. We find that the  $\tau$  values are reproducible to within an experimental uncertainty of 15%, and are the same to within the experimental uncertainty for both spontaneous and nucleated holes, as measured for films with  $h=209$  nm and  $h=253$  nm.

In Fig. 3, we plot the time constant  $\tau$  characterizing the hole growth rate as a function of the film thickness  $h$  for all of the films used in the present study. We observe a marked reduction in  $\tau$  with decreasing  $h$ , which can be understood in terms of the effect of shear strain rate  $\dot{\gamma}$  on the film viscosity  $\eta = \eta(\dot{\gamma}) = \sigma/\dot{\gamma}$ , where  $\sigma$  is the stress [13,14]. For small values of  $\dot{\gamma}$ ,  $\eta$  is equal to its zero shear strain rate value  $\eta_0$ , corresponding to the linear viscoelastic regime. However, for large values of  $\dot{\gamma}$ ,  $\eta$  decreases with increasing  $\dot{\gamma}$ , a nonlinear viscoelastic effect [13,14].

Holes in freely standing PS films grow with time because of the presence of a shear stress  $\sigma = 2\epsilon/h$  due to surface tension  $\epsilon$  at the edge of the hole (radial distance  $r = \mathcal{R}$ ). For PS at  $T=115$  °C,  $\epsilon = 34$  mN/m [15]. Because  $\sigma$  increases as  $h$  decreases, both  $\sigma$  and the resulting shear strain rate  $\dot{\gamma}$  can be large for very thin films. To understand the nature of the shear strain associated with the hole growth process, consider an infinitesimal square element of the film at  $r = \mathcal{R}$  with one of its diagonals along the radial direction, subtending the angular width  $d\theta$ . At a short time later, the same film element has moved outward to  $r = \mathcal{R} + d\mathcal{R}$ , and the element has been deformed into a parallelogram with its long diagonal perpendicular to the radial direction. We assume that the thickness of the film does not change. This is a reasonable approximation for the initial stages of hole growth because the hole radius is very small ( $\sim 10$   $\mu\text{m}$ ) compared to the in-plane extent of the film (4 mm), and the instantaneous elastic response of the viscoelastic film leads to uniform thickening [4,10]. The corresponding shear strain at the edge of the hole can be written as  $\gamma = 2(d\mathcal{R}/\mathcal{R})$ . Using Eq. (1),

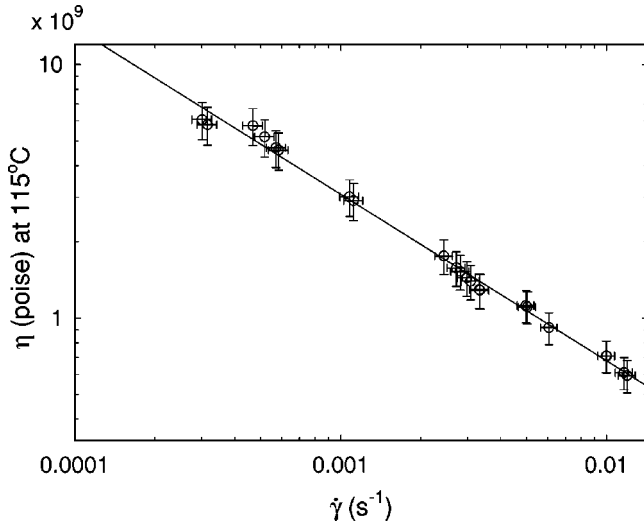


FIG. 4. Viscosity  $\eta$  at  $T = 115^\circ\text{C}$  versus the shear strain rate  $\dot{\gamma}$ . The straight line corresponds to the best fit to  $\eta \sim |\dot{\gamma}|^{-d}$ , with  $d = 0.65 \pm 0.03$ .

we obtain the shear strain rate at the edge of the hole as  $\dot{\gamma} = 2/\tau$ . Combining the above expressions for the shear stress  $\sigma$  and the shear strain rate  $\dot{\gamma}$ , we obtain an equation for the viscosity  $\eta$  at the edge of the hole (in agreement with Ref. [10]):

$$\eta = \frac{\sigma}{\dot{\gamma}} = \frac{\tau \epsilon}{h}. \quad (2)$$

From Fig. 2, one can see that, as  $h$  was decreased by a factor of 3.9, the measured  $\tau$  values decreased by a factor of 33. Given Eq. (2), the viscosity must decrease by an order of magnitude with decreasing  $h$  for the range of measured  $h$  values, if the surface tension  $\epsilon$  is the same for all films. It is reasonable to expect that  $\epsilon$  is the same for all films because  $h$  is large ( $>96$  nm for all films in the present study) compared with the length scale associated with surface tension ( $\sim 1$  nm [16]). Therefore, we ascribe the measured decrease in  $\tau/h$  with decreasing  $h$  to a decrease in  $\eta$  with decreasing  $h$ .

In Fig. 4 is shown a plot of  $\eta$  at  $T = 115^\circ\text{C}$  versus  $\dot{\gamma}$  for all of the films used in the present study. For each data point in Fig. 4, we have indicated error bars for the shear strain rate due to the uncertainty in the determination of  $\tau$ , as well as error bars for the viscosity due to the uncertainty in the sample temperature of  $\pm 0.5^\circ\text{C}$ . To make the conversion from uncertainty in temperature to uncertainty in viscosity, we have chosen a conservative estimate obtained by assuming that the Williams-Landel-Ferry (WLF) equation [17] applies for the present case. The error bars for the viscosity are consistent with the spread in the measured values. Clearly the results indicate a strong dependence of the viscosity on the shear strain rate produced during hole growth.

As discussed by Graessley [14], the importance of shear strain rate effects on the viscosity can be seen directly by calculating the dimensionless shear strain rate  $\beta \equiv \eta_0 \bar{M}_w \dot{\gamma} / \rho RT$ , where  $\eta_0$  is the zero shear rate viscosity,  $\rho$  is the density, and  $R$  is the gas constant. For bulk melts of PS with molecules of high molecular weight  $M_w$  and narrow

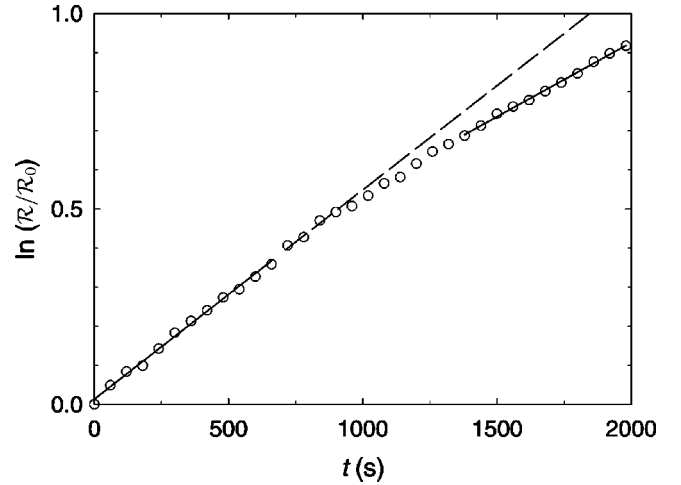


FIG. 5. Natural logarithm of the hole radius  $\mathcal{R}$ , normalized to the value of the radius  $\mathcal{R}_0$  first measured for the hole, as a function of time for a PS film with an initial thickness  $h = 209$  nm.

$M_w$  distributions, it has been found empirically that the *linear* viscoelastic regime, for which  $\eta = \eta_0$ , extends up to, at most,  $\beta \sim 10$  [14]. In the present study, the shear strain rates  $\dot{\gamma}$  ranged from  $3.01 \times 10^{-4} \text{ s}^{-1}$  to  $1.19 \times 10^{-2} \text{ s}^{-1}$  corresponding to  $\beta$  values ranging from  $\sim 40$  to  $\sim 1500$ . The  $\beta$  values were calculated using a value of  $\eta_0 \sim 6 \times 10^9$  P measured for bulk, high  $M_w$  PS at high temperature and extrapolated to  $T = 115^\circ\text{C}$  [17]. Because  $\beta$  is large for *all* films in the present study, we are probing the *nonlinear* viscoelastic regime for all films, as evidenced by the measured decrease in  $\eta$  with  $\dot{\gamma}$  (see Fig. 4).

For the nonlinear viscoelastic flow of a large number of different materials, it is found empirically that  $\eta \sim |\dot{\gamma}|^{-d}$ , with  $d \sim 0.85$  for bulk PS [14]. For our measurements of very thin, freely standing PS films, we obtain a best fit value of  $d = 0.65 \pm 0.03$  (see the solid line in Fig. 4). Our slightly lower value of  $d$  compared with those values obtained for bulk PS reveals the complicated nature of the hole growth experiment: if the measurement is performed in the nonlinear viscoelastic regime, the viscosity has a radial dependence in the vicinity of the hole edge because of the radial dependence of the shear strain rate. In particular, the viscosity is smallest at the hole edge ( $r = \mathcal{R}$ ), where the shear strain rate is largest, and the viscosity increases to  $\eta_0$  for large  $r$ , where the shear strain rate becomes negligible. Because we are measuring an average viscosity in the vicinity of the edge of the hole, the value of  $d$  measured in the present study should be less than that measured for bulk PS, which is in agreement with our experimental result.

Even though there is a radial dependence of  $\eta$  due to nonlinear viscoelastic effects in the present study, our results are consistent with uniform thickening of the films during the hole growth experiments. This is perhaps due to the instantaneous elastic response that leads to uniform thickening as in the linear viscoelastic case [4,10]. Because of the strong dependence of  $\tau$  on  $h$ , we can estimate the increase in  $h$  throughout the film during the hole growth experiment. In Fig. 5 we show  $\ln(\mathcal{R}/\mathcal{R}_0)$  versus time  $t$  for a PS film with an initial thickness of  $h = 209$  nm. The initial data can be used to obtain  $\tau = 1870$  s, corresponding to  $\eta = 3.0 \times 10^9$  P and

$\dot{\gamma}=1.07\times 10^{-3}\text{ s}^{-1}$  as shown in Fig. 4. With increasing time, a gradual decrease in the slope of  $\ln(\mathcal{R}/\mathcal{R}_0)$  versus  $t$  is observed, corresponding to an increase in  $\tau$  (a slower process) such that  $\tau=2640\text{ s}$  for  $1400\text{ s}<t<2000\text{ s}$ . We can estimate the film thickening that occurs during the hole growth experiment from a measurement of the area of the holes relative to the total sample area. For the sample of Fig. 5 for  $t=2000\text{ s}$  we obtain  $h\approx 230\text{ nm}$ . Using the late-stage values of  $h\approx 230\text{ nm}$  and  $\tau=2640\text{ s}$  ( $\dot{\gamma}=7.6\times 10^{-4}\text{ s}^{-1}$ ), Eq. (2) yields  $\eta\approx 3.9\times 10^9\text{ P}$ , which is consistent with the value interpolated from the initial-stage data shown in Fig. 4. This detailed analysis of the thickening of the films, together with the uniform color (and change in color) of all films measured during hole growth using optical microscopy, is consistent with uniform thickening of the films during hole growth. We emphasize that *all* of the data presented in Figs. 2–4 were obtained from the initial stages of hole growth for which the increase in film thickness was limited to less than 5%.

We have presented the results of measurements of hole formation and growth in freely standing polystyrene films. For all films, we observe that the hole radius grows exponentially with time, with uniform thickening of the films. The time constant  $\tau$  which characterizes the hole growth is found to decrease markedly with decreasing  $h$ . This effect can be understood in terms of reductions in the film viscosity produced by the large shear strain rates associated with the hole growth process. By extending previous linear viscoelastic studies of hole growth [4,10] to the nonlinear viscoelastic regime, we have obtained a novel probe of nonlinear viscoelastic effects in thin polymer films.

We thank F. Brochard-Wyart for helpful suggestions, G.B. McKenna and J.A. Forrest for critical comments on the manuscript, and C. Gigault for performing the ellipsometry measurements. The financial support of the Natural Sciences and Engineering Research Council (NSERC) of Canada is gratefully acknowledged.

- 
- [1] F. Brochard-Wyart and J. Daillant, *Can. J. Phys.* **68**, 1084 (1990).
  - [2] C. Redon, F. Brochard-Wyart, and F. Rondelez, *Phys. Rev. Lett.* **66**, 715 (1991).
  - [3] G. Reiter, *Phys. Rev. Lett.* **68**, 75 (1992).
  - [4] G. Debrégeas, P. Martin, and F. Brochard-Wyart, *Phys. Rev. Lett.* **75**, 3886 (1995).
  - [5] J.A. Forrest, K. Dalnoki-Veress, and J.R. Dutcher, *Phys. Rev. E* **56**, 5705 (1997).
  - [6] X. Zheng, M.H. Rafailovich, J. Sokolov, Y. Strzhemechny, S.A. Schwarz, B.B. Sauer, and M. Rubinstein, *Phys. Rev. Lett.* **79**, 241 (1997).
  - [7] E.K. Lin, W. Wu, and S.K. Satija, *Macromolecules* **30**, 7224 (1997).
  - [8] T.G. Stange, D.F. Evans, and W.A. Hendrickson, *Langmuir* **13**, 4459 (1997).
  - [9] A.N. Semenov, *Phys. Rev. Lett.* **80**, 1908 (1998).
  - [10] G. Debrégeas, P.-G. de Gennes, and F. Brochard-Wyart, *Science* **279**, 1704 (1998).
  - [11] J.A. Forrest, C. Svanberg, K. Revesz, M. Rodahl, L.M. Torell, and B. Kasemo, *Phys. Rev. E* **58**, R1226 (1998).
  - [12] C.V. Boys, *Soap Bubbles* (Dover, New York, 1959).
  - [13] G. Strobl, *The Physics of Polymers*, 2nd ed. (Springer, Berlin, 1997).
  - [14] W.W. Graessley, *Adv. Polym. Sci.* **16**, 1 (1974).
  - [15] *Polymer Handbook*, 3rd ed., edited by J. Brandrup and E.H. Immergut (Wiley, New York, 1989).
  - [16] G.T. Dee and B.B. Sauer, *J. Colloid Interface Sci.* **152**, 85 (1992).
  - [17] K.L. Ngai and D.J. Plazek, in *Physical Properties of Polymers Handbook*, edited by J.E. Mark (AIP, Woodbury, NY, 1996), Chap. 25.